Energy flow in angularly dispersive optical systems

M. Ware, W. E. Dibble, S. A. Glasgow, and J. Peatross

Dept. of Physics and Astronomy, Brigham Young University, Provo, Utah 84602

Received September 18, 2000

Light-pulse propagation in angularly dispersive systems is explored in the context of a center-of-mass definition of energy arrival time. In this context the time of travel is given by a superposition of group delays weighted by the spectral content of the pulse. With this description the time of travel from one point to the next for a pulse is found to be completely determined by the spectral content, independent of the state of chirp. The effect of sensor orientation on arrival time is also considered. © 2001 Optical Society of America

OCIS codes: 260.2160, 050.1590, 350.5030.

1. INTRODUCTION

Angularly dispersive optical systems are routinely employed in short-pulse lasers to control the temporal profile of pulses and to mitigate unwanted dispersion.[1–3] Such systems include grating pairs, prism pairs, and material slabs that are angularly dispersive (within the material) under oblique incidence. An interesting aspect of pulse propagation within an angularly dispersive system is the time that it takes for the energy of a pulse to traverse the system. Indeed, arguments based on the energy transport's taking place at the group velocity have been used to produce the required form of the frequency-dependent phase delay in such systems.[4] Until recently the concept of group velocity has been associated with a narrow-band context. However, as laser pulses are made to have increasingly shorter durations it becomes interesting to consider these issues in a general broadband context. In another paper[5] we introduced a theorem placing group velocity into a general broadband context and applied it to the problem of anomalous dispersion in the case of collinear propagation. In the present paper we apply the theorem to angularly dispersive systems.

As the frequency components composing a pulse travel in different directions within an angularly dispersive system, dispersion can cause the pulse shape and duration to evolve in complicated and asymmetric ways. This makes the concept of energy transport time somewhat vague unless pulse arrival time is carefully defined. In this paper we use a temporal expectation integral of the energy reaching a sensor at a chosen location to specify the pulse arrival time. Within this context the pulse propagation time is closely connected to a linear superposition of group delays (inverse of group velocity) weighted by the spectral content of the pulse. The concept of group velocity enters the picture without our resorting to a perturbative expansion about a carrier frequency. The analysis is appropriate for pulses of arbitrarily wide bandwidth.

2. PHASE DELAY IN DISPERSIVE SYSTEMS

The form of a pulse at various points in a dispersive system may be found by use of the phase delay function

$$\phi(\omega) = \mathbf{k}(\omega) \cdot \Delta\mathbf{r}. \tag{1}$$

The wave vector $\mathbf{k}(\omega)$ specifies the direction of travel for each frequency, and the displacement $\Delta\mathbf{r} \equiv \mathbf{r} - \mathbf{r}_0$ represents the separation between a point $\mathbf{r}_0$, where the form of the pulse is known, and a point $\mathbf{r}$, where the form of the pulse is to be found. For simplicity we assume a single wave vector for each frequency. Thus diffraction effects associated with narrow beams[6] are ignored, but this approximation is reasonable for many optical systems (e.g., compression of large beams). The phase-delay function $\phi(\omega)$ gives the difference in phase between the field at $\mathbf{r}_0$ and at $\mathbf{r}$ for each frequency component. The form of the pulse at $\mathbf{r}$ is then

$$\mathbf{E}(\mathbf{r}, t) = \frac{1}{\sqrt{2\pi}} \int_{-\infty}^{\infty} \mathbf{E}(\mathbf{r}_0, \omega) \exp[i\phi(\omega)] \exp(-i\omega t) \mathrm{d}\omega, \tag{2}$$

where the frequency representation of the field at $\mathbf{r}_0$ is found from the usual Fourier transform

$$\mathbf{E}(\mathbf{r}_0, \omega) = \frac{1}{\sqrt{2\pi}} \int_{-\infty}^{\infty} \mathbf{E}(\mathbf{r}_0, t) \exp(i\omega t) \mathrm{d}t. \tag{3}$$

The method of finding phase delay in angularly dispersive systems represented in Eq. (1) was used by Martinez *et al.*[7] A related method sometimes employed is to trace a representative ray for an arbitrary frequency as it traverses the system. The phase delay is then computed as $\phi(\omega) = k(\omega) l(\omega)$, where $l(\omega)$ is the frequency-dependent path length and the vectoral nature of the wave number is suppressed. The results derived in this manner are fairly straightforward for dielectric media such as prism pairs and material windows, although the geometry is cumbersome. In the case of parallel gratings, Treacy[8] showed that it is necessary to append a phase-matching term to the phase delay obtained by the representative-ray method in order to arrive at the correct result. We find it more convenient to utilize the vectoral nature of $\mathbf{k}(\omega)$ as in Eq. (1) when calculating the phase delay of an angularly dispersive setup. This

method avoids the need for phase-matching terms associated with diffraction and also avoids much of the geometry necessary in the representative-ray approach. For the representative-ray method to yield a tenable result, $l(\omega)$ must begin and end on planes that are parallel to the wave fronts for all frequencies chosen before the wave front enters and after it exits the system. However, the phase delay in Eq. (1) can be calculated between arbitrary points *within* a system (e.g., at points between grating pairs) where it is not possible to define a plane parallel to the wave fronts for all frequencies.

In many systems the angular spread of $\mathbf{k}(\omega)$ is confined to a plane, say the x–y plane. In this case the wave vector may be represented as

$$\mathbf{k}(\omega) = k[\hat{x}\cos\theta(\omega) + \hat{y}\sin\theta(\omega)], \tag{4}$$

where $\theta(\omega)$ is the direction of travel for each frequency component referenced to the x axis as depicted in Fig. 1(a). [Recall that we have assumed a single wave vector per frequency.] For a displacement $\Delta\mathbf{r} \equiv \hat{x}\Delta x + \hat{y}\Delta y$ as depicted in Fig. 1(b), Eqs. (1) and (4) combine to yield

$$\begin{aligned}\phi(\omega) &= \mathbf{k}(\omega)\cdot\Delta\mathbf{r} \\ &= [\omega n(\omega)/c][\Delta x\cos\theta(\omega) + \Delta y\sin\theta(\omega)],\end{aligned} \tag{5}$$

where we have incorporated the dispersion relation in an isotropic medium: $k(\omega) = n(\omega)\omega/c$. The specification of the frequency dependence of $\theta(\omega)$ necessarily contains the essential geometry for a given angularly dispersive system. Thus it is only necessary to know the direction of travel of each frequency component to calculate the phase delay. In Appendix A we give the forms of $\theta(\omega)$ and use Eq. (5) to calculate $\phi(\omega)$ for a grating, a prism, and a dielectric interface. In these systems it is assumed that all frequencies travel in parallel before meeting the particular element. In typical setups a second grating, a prism, or a dielectric interface reorients the wave vectors to travel in parallel again. The phase delays for these systems are well known (e.g., Ref. 9), but Appendix A is included as a reference for use with the formalism in this paper.

3. GROUP DELAY IN DISPERSIVE SYSTEMS

In Treacy's original paper on parallel-grating systems, the argument for the phase-matching term appended to the representative-ray approach is subtle and connected with the specific geometry of the gratings. This prompted Brorson and Haus[4] to reexamine the setup in terms of an energy transport argument involving the group velocity, which obtained the required derivative of the phase delay with less reliance on specific geometry and without the need for appending a phase-matching term. They first showed that the well-known diffraction grating law [describing a diffracted angle in terms of the incidence angle and groove spacing, Eq. (A1)] is derivable by variational methods. Their argument states that, since energy transport must occur at velocity c (assuming vacuum between gratings) along the path predicted by variational methods, the *group-delay function* $\partial\phi(\omega)/\partial\omega$ must be equal to $l(\omega)/c$, where $l(\omega)$ is the frequency-dependent path length through the grating system as used by Treacy. This argument has its own subtleties, since the variational method (justified by the eikonal equation[10]) applies to individual frequencies, whereas $\partial\phi(\omega)/\partial\omega$ necessarily involves neighboring frequencies.

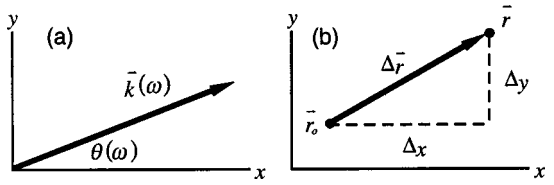

Fig. 1. (a) Orientation of $\mathbf{k}(\omega)$ assumed to lie in the x–y plane. (b) Displacement $\Delta\mathbf{r}$ between points $\mathbf{r}_0$ and $\mathbf{r}$ where pulse forms will be examined.

In traditional pedagogy[10] group delay is often introduced in the context of an expansion of the phase delay about a carrier frequency $\bar{\omega}$:

$$\begin{aligned}\phi(\omega) \approx \phi(\omega)|_{\bar{\omega}} &+ \left.\frac{\partial\phi(\omega)}{\partial\omega}\right|_{\bar{\omega}}(\omega-\bar{\omega}) \\ &+ \left.\frac{1}{2}\frac{\partial^2\phi(\omega)}{\partial\omega^2}\right|_{\bar{\omega}}(\omega-\bar{\omega})^2 + \cdots.\end{aligned} \tag{6}$$

The linear coefficient $\partial\phi(\omega)/\partial\omega|_{\bar{\omega}}$ is recognized as the group delay but evaluated at only a single frequency. To first order, this term describes the time that it takes the pulse to travel from $\mathbf{r}_0$ to $\mathbf{r}$. However, the coefficients of the Taylor's series depend on the choice of carrier frequency $\bar{\omega}$, thus affecting this first-order approximation of energy transport time. Moreover, higher-order terms in the phase-delay expansion also influence the energy transport time to the extent that the pulse shape evolves asymmetrically. It is therefore essential that the analysis of Brorson and Haus[4] require $\partial\phi(\omega)/\partial\omega$ to be evaluated at each frequency rather than at a single carrier frequency as in relation (6). Thus a linear-superposition principle for group delays is implied by their conclusion, although this fact was not emphasized in Ref. 4. This superposition principle will be demonstrated explicitly in Section 4.

Before proceeding, we briefly explore Eq. (5) in a special case relevant to the Brorson and Haus analysis, which addressed one frequency at a time yet invoked the multifrequency concept of group delay. To obtain the group delay along a path parallel to the wave vector of a specific frequency ω', we may differentiate Eq. (5) with the displacement chosen to be parallel to $\mathbf{k}(\omega')$. A displacement $\Delta\mathbf{r}$ in this direction corresponds to the vector components

$$\Delta x = \Delta r\cos\theta(\omega'), \qquad \Delta y = \Delta r\sin\theta(\omega'). \tag{7}$$

Substitution of Eqs. (7) into Eq. (5) yields simply

$$\left.\frac{\partial\phi}{\partial\omega}\right|_{\omega'} = \frac{\Delta r}{c}\left[n(\omega') + \left.\frac{\partial n}{\partial\omega}\right|_{\omega'}\right]. \tag{8}$$

As expected, this group delay (evaluated at ω') reduces to $\Delta r/c$ for propagation in vacuum. Thus the group delay evaluated at individual frequencies taken along their respective paths occurs at the speed of light *regardless of the functional form of* $\theta(\omega)$, and in particular $\theta(\omega)$ need

not be derivable from variational methods. This seemingly contradicts the emphasis placed on variational methods by Brorson and Haus in the case of a grating pair. However, the fact that the grating dispersion formula is derivable from variational principles means that energy does not linger (or advance in time) on the grating surfaces during the act of reflection, which is critical to their argument.

4. ENERGY TRANSPORT TIME AND GROUP DELAY

We next turn our attention to the connection between energy transport time and group delay. In a dispersive system, pulse shape may evolve in complicated ways during propagation, especially if the spectrum is broad. As was mentioned in Section 3, the second term in relation (6) is insufficient for determining the delay of the pulse except in a narrow-band situation, and we will not use this expansion. To specify the energy transport time of arbitrary pulses, it is necessary to define the pulse arrival time at a point in a way that is insensitive to the specific features of the pulse temporal profile. As an example of the need for caution, the peak of the pulse is not a good choice to indicate arrival time, since energy may be asymmetrically distributed about the peak or there may be multiple peaks. The method that we employed in Ref. 5 defines the time of arrival for a pulse at a point as a temporal expectation, which is weighted by the energy transport flux. The energy transport flux is given by the Poynting vector, $\mathbf{S}(\mathbf{r}, t) = \mathbf{E}(\mathbf{r}, t) \times \mathbf{H}(\mathbf{r}, t)$ where $\mathbf{E}$ and $\mathbf{H}$ are the real electric and magnetic fields. The time of arrival at $\mathbf{r}$ is written as

$$\langle t \rangle_{\mathbf{r}} \equiv \hat{u} \cdot \int_{-\infty}^{\infty} t\mathbf{S}(\mathbf{r}, t)\mathrm{d}t \Big/ \hat{u} \cdot \int_{-\infty}^{\infty} \mathbf{S}(\mathbf{r}, t)\mathrm{d}t, \qquad (9)$$

which may be viewed as a kind of temporal center-of-mass. The unit vector $\hat{u}$ specifies the orientation of a "sensor" at $\mathbf{r}$ that detects the incoming energy flux. In an angularly dispersive system the orientation of this energy sensor influences arrival time for the pulse, since different frequency components may illuminate the sensor closer to or farther from normal incidence, as will be illustrated in Section 5.

Using the definition of temporal position given in Eq. (9), it is shown in Ref. 5 that the time $\Delta t \equiv \langle t \rangle_{\mathbf{r}} - \langle t \rangle_{\mathbf{r}_0}$ from when a pulse passes a position $\mathbf{r}_0$ until it arrives at $\mathbf{r} = \mathbf{r}_0 + \Delta\mathbf{r}$ can be written as the spectral average of the group delays of individual frequency components. We assume that there is no material interface or reflection that the light experiences between $\mathbf{r}_0$ and $\mathbf{r}$ (i.e., $\mathbf{k}(\omega)$ remains constant). The travel time Δt can be expressed as

$$\Delta t = \hat{u} \cdot \int_{-\infty}^{\infty} \mathbf{S}(\mathbf{r}_0, \omega) \frac{\partial \phi(\omega)}{\partial \omega} \mathrm{d}\omega \Big/ \hat{u} \cdot \int_{-\infty}^{\infty} \mathbf{S}(\mathbf{r}_0, \omega)\mathrm{d}\omega, \qquad (10)$$

where $\mathbf{S}(\mathbf{r}, \omega)$ is the Poynting vector obtained in the usual manner from Fourier transforms of the electric and magnetic fields. This expression must be modified in the case of absorption, as explained in Ref. 5, but for the current consideration we neglect absorption. An outline of the derivation of this theorem for the nonabsorbing case is given in Appendix B. The striking similarity between Eq. (9) and Eq. (10) is immediately evident. The time expectation integral in Eq. (9) leads to the group-delay expectation integral in Eq. (10). The total delay between the pulse crossing points $\mathbf{r}_0$ and $\mathbf{r}$ is given by a linear superposition of the group delay at every frequency weighted by the spectral content of the pulse. This result is insensitive to the specific temporal organization of the pulse for a given spectrum. Equation (10) demonstrates the linear-superposition principle of group delay that is implicit in the Brorson and Haus argument, as previously mentioned.

5. DETECTION ANGLE AND ENERGY TRANSPORT TIME

In this section we examine the effect of sensor orientation on the arrival time of the pulse in angularly dispersive systems where the direction of the wave vectors depends on frequency. Consider a grating pair, a material slab, or a prism pair as outlined in Appendix A. We assume that all frequencies associated with the initial pulse travel in a single direction before entering the system, indicated by θ_i. The spectral components of the field within the interior of the angularly dispersive system can be written in terms of the initial field amplitude as follows:

$$\mathbf{E}(\omega, \mathbf{r}) = E_i(\omega, \mathbf{r}_0)\sqrt{\xi}(-\sin\theta\hat{x} + \cos\theta\hat{y})\exp[i\phi(\omega)], \qquad (11)$$

$$\mathbf{H}(\omega, \mathbf{r}) = \frac{k}{\mu_0\omega} E(\omega, \mathbf{r})\hat{z}, \qquad (12)$$

where we have assumed p-polarized light propagating in the x–y plane. $E_i(\omega, \mathbf{r}_0)$ is the field spectrum incident upon the system. The point $\mathbf{r}_0$ is taken to lie on the first grating surface in the case of a grating pair, on the dielectric interface in the case of a material slab, or at the apex of the first prism in the case of a prism pair.

The parameter ξ contains the factors related to the efficiency of transferring energy into the system. In the case of a grating pair, ξ is equal to the diffraction efficiency (possibly frequency dependent) multiplied by the ratio $\cos\theta_i/\cos\theta$, a geometrical factor arising from the change in propagation direction as the pulse enters the system. For the grating we ignore frequency-dependent phase effects associated with the reflection from the grating material, which would modify the incident field $E_i(\omega, \mathbf{r}_0)$. In the case of a material slab, ξ is equal to the surface transmittance $T \equiv \cos\theta_i|t|^2/n\cos\theta$, where t is the Fresnel transmission coefficient. For a prism pair, the passing of the pulse through the first prism gives for ξ the product of the transmittances of the two prism surfaces. It is important to note that in each system the geometrical factors are removed at the second element, whereupon the various frequency components are redirected into a common direction parallel to the propagation direction of the incident pulse. However, the spectral content of the pulse is irreversibly modified to the extent that diffraction efficiency or the Fresnel transmittance coefficients have a strong frequency dependence.

The spectral representation of the Poynting vector from Eqs. (11) and (12) becomes

$$\mathbf{S}(\omega, \mathbf{r}) \equiv \mathbf{E}(\omega, \mathbf{r}) \times \mathbf{H}^*(\omega, \mathbf{r})$$

$$= \xi |E_i(\omega, \mathbf{r}_0)|^2 \frac{k}{\mu_0 \omega} [\cos\theta \hat{x} + \sin\theta \hat{y}], \quad (13)$$

which is independent of position $\mathbf{r}$. In the case of a grating, to the extent that the diffraction efficiency is uniform over frequency, Eq. (13) reveals that for the specific sensor orientation $\hat{u} = \hat{x}$ (i.e., the sensor is parallel to the grating surface), projection of the energy flow onto the sensor carries the identical spectral profile as the initial pulse before encountering the grating. (To see this, note that ξ is inversely proportional to $\cos\theta$.) To the extent that the sensor angle is oriented differently, the spectral content of the pulse arriving at the sensor is altered. In typical systems, such as grating pairs employed in laser systems, this effect is not dramatic, since the range of angles present is typically rather modest (a few degrees).

To illustrate how detection angle affects the perceived delay time, we consider a Gaussian pulse given by

$$\mathbf{E}(\mathbf{r}_0, t) = \mathbf{E}_0 \exp(-t^2/\tau^2) \exp(-i\omega_0 t)$$

as it diffracts from a grating surface. Figure 2(a) shows a two-dimensional plot of the intensity at $t = 0$ for a pulse with width $\tau = 5$ fs, and ω_0 chosen to correspond with a vacuum wavelength of 800 nm. The incoming pulse strikes the grating surface at an angle of 20° from normal incidence, and the line spacing is chosen to be 1/1200 mm. The spatial dimensions of Fig. 2(a) are 0.5 mm wide and 1 mm tall. For reference, the incoming pulse is also shown. Arrows show the direction of the wave vector associated with the center frequency ω_0. Figure 2(b) shows the direction of the Poynting vector at each point of the intensity distribution (points with an intensity less than 10^{-4} in Fig. 2(a) are set to black). As time proceeds, the intensity and direction patterns slide vertically downward along the grating surface while maintaining their forms. The Poynting vector changes direction in time as the wave form crosses a given point. This change in direction is a general feature of a chirped pulse in an angularly dispersive system and influences the efficiency of detecting the pulse during passage. Nevertheless, the pulse propagation time [i.e., the difference in arrival times at $\mathbf{r}$ and $\mathbf{r}_0$ as given by Eq. (10)] is impervious to this. In other words, the direction of the Poynting vector evolves in time in such a way as to counteract asymmetries in the chirping process, so that propagation time as noted by the sensors at $\mathbf{r}$ and $\mathbf{r}_0$ is independent of the state of chirp. For this to be true it is important that the orientation of the two sensors match, since this was assumed in deriving Eq. (10).

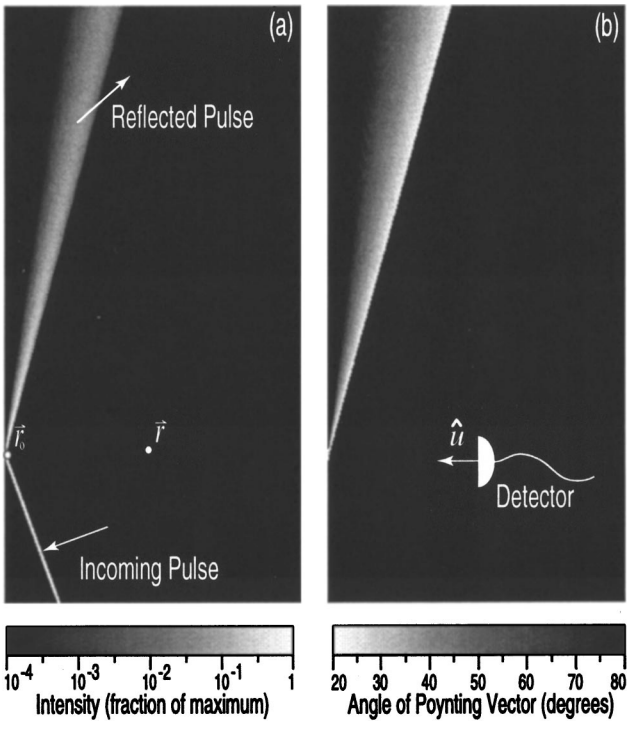

Fig. 2. (a) Snapshot of the intensity distribution of a Gaussian pulse diffracting from a grating surface. (b) Angle of the Poynting vector, measured from the horizontal x axis, for the pulse illustrated in (a).

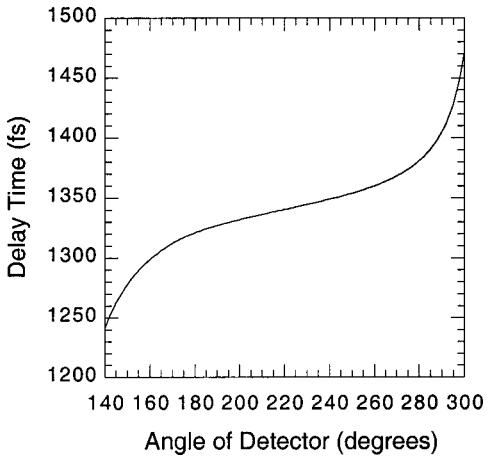

Fig. 3. Pulse delay time from $\mathbf{r}_0$ to $\mathbf{r}$ as a function of detector orientation, $\hat{u}$, for the system illustrated in Fig. 2. The angle is measured from the horizontal x axis.

Figure 3 shows the delay time, as a function of sensor angle, for the pulse illustrated in Fig. 2 to travel from point $\mathbf{r}_0$ to another $\mathbf{r}$ after diffracting from the grating. The angles are measured from the a horizontal x axis, and we have chosen $\Delta\mathbf{r}$ to be 0.25 mm in the $\hat{x}$ direction (points are illustrated in Fig. 2). The delay time increases as the detector rotates counterclockwise and becomes less sensitive to wave vectors directed closer to the grating normal. In generating this plot, we have considered the detector to be sensitive on only one side, so that contributions to the integrals in Eq. (10) with a positive dot product were ignored. This effect is not important when the detector is oriented roughly toward the grating. While the sensor angle plays a significant role in determining the center-of-mass propagation time associated with traversing $\Delta\mathbf{r}$, the result is not influenced by the state of the pulse's chirp, as was previously mentioned. Whether the pulse begins relatively compressed and then incurs chirp, begins with a negative chirp that compresses, or begins with a positive chirp that becomes more

pronounced during propagation, the travel time of the center of mass is the same.

These results are not surprising from the point of view that the Poynting vector in its frequency representation is insensitive to the phases of the individual spectral field components. Therefore the propagation time for the pulse to traverse $\Delta\mathbf{r}$ cannot recognize the presence of chirp within the context of Eq. (10). This would still be the case even if the sensor were insensitive to the incident angle of the radiation and were able to absorb radiation equally well from any direction (i.e., if the unit vector $\hat{u}$ were removed from Eq. (10) and the Poynting vector were replaced with its magnitude). In this hypothetical case the delay time assigned to pulse propagation would still be insensitive to chirp. Nevertheless, the result for the delay would be different from that in the case of the directional sensor, since the integrand in Eq. (10) would vary in the two cases.

6. SUMMARY

In this paper we have examined the propagation of energy in angularly dispersive systems. We demonstrated explicitly that, under the center-of-mass definition of arrival time, the time it takes for a pulse to propagate from one point to another is simply a spectral superposition of the group delay for each frequency weighted by the spectral content of the pulse. Since this approach does not involve approximating the phase-delay function, it retains validity for pulses of arbitrarily wide bandwidth. We have also investigated the effects of sensor orientation on pulse arrival time. When the sensors that perceive a pulse are oriented in the same direction at the beginning and the end of propagation, the time of travel depends on the spectral content of a pulse but not its temporal organization. Thus the state of chirp does not affect the total delay.

APPENDIX A: PHASE DELAY FOR THE DIFFRACTION GRATING PAIR, DIELECTRIC WINDOW, AND PRISM PAIR

For the diffraction grating pair it is convenient to apply Eq. (5) by orienting the system so that the gratings are parallel to the y axis. We choose our initial reference point, $\mathbf{r}_0$, on the first diffraction grating surface as shown in Fig. 4(a). For first-order diffraction the direction of travel, given by $\theta(\omega)$, is readily obtained from the well-known diffraction grating law

$$\theta_g(\omega) = \sin^{-1}\left(\frac{2\pi c}{\omega d} - \sin\theta_i\right), \tag{A1}$$

where θ_i is the incident angle and d is the grating line spacing. If we are interested in only the form of the final pulse as opposed to its arrival time, we may evaluate the field at any point on the second grating, since after the bounce from the second grating the direction of travel for the various frequencies is the same as before the first bounce. A convenient point for evaluating the phase delay is directly across from $\mathbf{r}_0$, so that $\Delta\mathbf{r} = l_g\hat{x}$, where l_g is the separation between the gratings. We may then immediately write the phase delay, by using Eq. (5), as

$$\phi_g(\omega) = l_g\frac{\omega}{c}\left[1 - \left(\frac{2\pi c}{\omega d} - \sin\theta_i\right)^2\right]^{1/2}, \tag{A2}$$

where we have employed the identity $\cos[\sin^{-1}(x)] = (1 - x^2)^{1/2}$.

We next consider a dielectric window at an arbitrary incidence angle, oriented parallel to the y axis shown in Fig. 4(b). The direction of travel is easily obtained by use of Snell's law:

$$\theta_w(\omega) = \sin^{-1}\left[\frac{\sin\theta_i}{n(\omega)}\right]. \tag{A3}$$

We choose $\mathbf{r}_0$ to be a point on the window's first surface and evaluate the phase delay at a point directly across from $\mathbf{r}_0$, so that $\Delta\mathbf{r} = l_w\hat{x}$, where l_w is the thickness of the window. Again, Eq. (5) immediately gives the phase delay for the complete element:

$$\phi_w(\omega) = l_w\frac{\omega}{c}[n(\omega)^2 - \sin^2(\theta_i)]^{1/2}. \tag{A4}$$

In practice, the effects of angular dispersion introduced by traversing the slab are small compared with the dispersion of the material itself. For example, for 800-nm light incident at Brewster's angle on a 1-cm-thick Ti:sapphire crystal, the third derivative of the phase delay obtained in Eq. (A4) differs by less than 1% from that

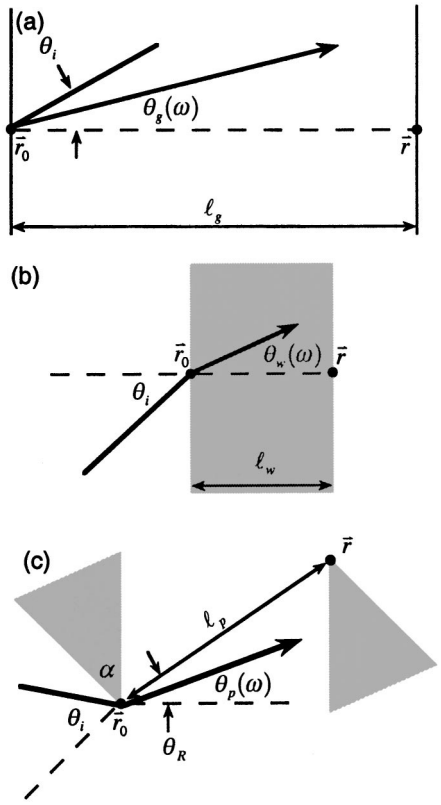

Fig. 4. Geometry for (a) diffraction grating pair, (b) material window, and (c) prism pair.

calculated when the angular dispersion is ignored and the light is treated as being at normal incidence on a slab with thickness $l_w/\cos\theta_w(\omega)$.

For the prism pair it is convenient to orient the system so that the interior faces of the prisms are parallel to the y axis as shown in Fig. 4(c). With two applications of Snell's law, we can calculate the direction of travel as

$$\theta_p(\omega) = \sin^{-1}\left(n(\omega)\sin\left\{ \alpha - \sin^{-1}\left[\frac{\sin\theta_i}{n(\omega)}\right]\right\}\right), \quad \text{(A5)}$$

where θ_i is the angle of incidence on the first prism surface and α is the apex angle. For a standard double-prism configuration, a convenient place to evaluate the phase delay is between the apices of the two prisms, since these will match the form of the pulse on the exterior sides of the prism. We could evaluate the pulse at any other two points on the sides of the prisms, but then the effect of propagation through the interior of the prism would also need to be considered. We define $\mathbf{r}_0$ to be at the apex of the first prism so that $\Delta\mathbf{r} = l_p\cos(\theta_R)\hat{x} + l_p\sin(\theta_R)\hat{y}$, where l_p is the distance between prism apices and θ_R is the angle between the line connecting the two apices and the normal to the interior faces of the prisms. Applying these parameters to Eq. (5), we calculate the phase delay:

$$\phi_p(\omega) = l_p\frac{\omega}{c}\cos[\theta_R - \theta_p(\omega)]. \quad \text{(A6)}$$

This method is essentially the same as the equivalent optical-path method used by Fork *et al.*[11] but requires much less geometry. We can verify that this formula correctly includes the dispersion introduced by propagation through the prism interior by allowing the two prisms to touch, as was pointed out by Durfee *et al.*[3] In this case we have $\theta_R = \pi/2$ and $l_w = l_p\sin\alpha$, whereupon Eq. (A6) is quickly reduced to Eq. (A4), aside from a linear frequency delay consistent with the different orientations of the two setups.

APPENDIX B: DERIVATION OF ENERGY TRANSPORT TIME IN DISPERSIVE SYSTEMS

In this appendix we derive an expression for the time it takes for a pulse to travel between two points under the center-of-mass definition of arrival in the nonabsorbing case. The time of arrival at a point $\mathbf{r}$ was given in Eq. (9):

$$\langle t\rangle_{\mathbf{r}} \equiv \hat{u}\cdot\int_{-\infty}^{\infty} t\mathbf{S}(\mathbf{r},t)\mathrm{d}t \Big/ \hat{u}\cdot\int_{-\infty}^{\infty}\mathbf{S}(\mathbf{r},t)\mathrm{d}t. \quad \text{(B1)}$$

The denominator in Eq. (B1) is transformed to the frequency domain via Parsevall's theorem [i.e., $\int_{-\infty}^{\infty}\mathbf{S}(\mathbf{r},t)\mathrm{d}t = \int_{-\infty}^{\infty}\mathbf{S}(\mathbf{r},\omega)d\omega$]. The numerator in Eq. (B1) may be transformed by our writing the Poynting vector in terms of its field spectra. After reordering integration and introducing a partial derivative to account for the factor t, the numerator becomes

$$-i\hat{u}\cdot\int_{-\infty}^{\infty}\mathbf{H}(\mathbf{r},\omega)\mathrm{d}\omega \times\frac{\partial}{\partial\omega}\int_{-\infty}^{\infty}\mathbf{E}(\mathbf{r},\omega')\mathrm{d}\omega'\left[\frac{1}{2\pi}\int_{-\infty}^{\infty}\exp[-i(\omega+\omega')t]\mathrm{d}t\right]. \quad \text{(B2)}$$

The time integral enclosed in brackets yields the delta function $\delta(\omega+\omega')$. This result is used along with the fact that the fields were strictly real in the time domain to arrive at the final form for $\langle t\rangle_{\mathbf{r}}$:

$$\langle t\rangle_{\mathbf{r}} = -i\hat{u}\cdot\int_{-\infty}^{\infty}\frac{\partial\mathbf{E}(\mathbf{r},\omega)}{\partial\omega}\times\mathbf{H}^*(\mathbf{r},\omega)\mathrm{d}\omega \Big/ \hat{u}\cdot\int_{-\infty}^{\infty}\mathbf{S}(\mathbf{r},\omega)\mathrm{d}\omega. \quad \text{(B3)}$$

To obtain delay time $\Delta t \equiv \langle t\rangle_{\mathbf{r}} - \langle t\rangle_{\mathbf{r}_0}$ we need to relate the fields at $\mathbf{r}_0$ with those at $\mathbf{r}$. This is accomplished by using the phase delay discussed in Section 2:

$$\mathbf{E}(\mathbf{r},\omega) = \mathbf{E}(\mathbf{r}_0,\omega)\exp[i\phi(\omega)],$$
$$\mathbf{H}(\mathbf{r},\omega) = \mathbf{H}(\mathbf{r}_0,\omega)\exp[i\phi(\omega)]. \quad \text{(B4)}$$

The expressions in Eq. (B4) are inserted into Eq. (B3), and the partial derivative is evaluated to obtain an expression for $\langle t\rangle_{\mathbf{r}}$ in terms of the fields at $\mathbf{r}_0$:

$$\langle t\rangle_{\mathbf{r}} = \hat{u}\cdot\int_{-\infty}^{\infty}\left[-i\frac{\partial\mathbf{E}(\mathbf{r}_0,\omega)}{\partial\omega} + \mathbf{E}(\mathbf{r}_0,\omega)\frac{\partial\phi(\omega)}{\partial\omega}\right] \times\mathbf{H}^*(\mathbf{r}_0,\omega)\mathrm{d}\omega \Big/ \hat{u}\cdot\int_{-\infty}^{\infty}\mathbf{S}(\mathbf{r}_0,\omega)\mathrm{d}\omega. \quad \text{(B5)}$$

From this expression it is straightforward to evaluate the delay time to obtain the result given in Eq. (10):

$$\Delta t \equiv \langle t\rangle_{\mathbf{r}} - \langle t\rangle_{\mathbf{r}_0} = \hat{u}\cdot\int_{-\infty}^{\infty}\mathbf{S}(\mathbf{r}_0,\omega)\frac{\partial\phi(\omega)}{\partial\omega}\mathrm{d}\omega \Big/ \hat{u}\cdot\int_{-\infty}^{\infty}\mathbf{S}(\mathbf{r}_0,\omega)\mathrm{d}\omega. \quad \text{(B6)}$$

M. Ware may be reached at mw22@email.byu.edu.

REFERENCES

1. M. Pessot, P. Maine, and G. Mourou, "1000 times expansion/compression of optical pulses for chirped pulse amplification," Opt. Commun. **62**, 419–421 (1987).
2. D. N. Fittinghoff, B. C. Walker, J. A. Squier, C. S. Toth, C. Rose-Petruck, and C. P. J. Barty, "Dispersion considerations in ultrafast CPA systems," IEEE J. Sel. Top. Quantum Electron. **4**, 430–440 (1998).
3. C. G. Durfee III, S. Backus, M. M. Murnane, and H. C. Kapteyn, "Design and implementation of a TW-class high-average power laser system," IEEE J. Sel. Top. Quantum Electron. **4**, 395–405 (1998).
4. S. D. Brorson and H. A. Haus, "Diffraction gratings and geometric optics," J. Opt. Soc. Am. B **5**, 247–248 (1988).
5. J. Peatross, S. A. Glasgow, and M. Ware, "Average energy flow of optical pulses in dispersive media," Phys. Rev. Lett. **84**, 2370–2373 (2000).
6. O. E. Martinez, "Grating and prism compressors in the case of finite beam size," J. Opt. Soc. Am. B **3**, 929–934 (1986).
7. O. E. Martinez, J. P. Gordon, and R. L. Fork, "Negative

group-velocity dispersion using refraction," J. Opt. Soc. Am. A **1**, 1003–1006 (1984).
8. E. B. Treacy, "Optical pulse compression with diffraction gratings," IEEE J. Quantum Electron. **QE-5**, 454–458 (1969).
9. C. H. Brito Cruz, P. C. Becker, R. L. Fork, and C. V. Shank, "Phase correction of femtosecond optical pulses using a combination of prisms and gratings," Opt. Lett. **13**, 123–125 (1988).
10. M. Born and E. Wolf, *Principles of Optics*, 7th ed. (Cambridge U. Press, Cambridge, U.K., 1999), pp. 117–119.
11. R. L. Fork, O. E. Martinez, and J. P. Gordon, "Negative dispersion using pairs of prisms," Opt. Lett. **9**, 150–152 (1984).